Microwave Band-Stop Filters With Narrow Stop Bands*

L. YOUNG†, SENIOR MEMBER, IRE, G. L. MATTHAEI†, MEMBER, IRE, AND
E. M. T. JONES‡, SENIOR MEMBER, IRE

Summary—Band-stop filters can be used to eliminate a band of frequencies, or to separate such a band from other frequencies; if properly designed, the insertion loss at frequencies outside the stop-band can be minimized. The filters considered here have stop-band bandwidths up to a few per cent, and equiripple or maximally flat characteristics in the passband. Design formulas are presented. The effect of dissipation loss is included. A strip-line filter and a waveguide filter were constructed. Experimental results conform closely to the performance predicted by theory.

I. INTRODUCTION

IN MOST MICROWAVE systems the signal frequency has to be transmitted and guided from one place to another with a minimum of attenuation, while guarding against unwanted frequencies by keeping them out with band-pass filters, which pass only the signal frequency. The common types of band-pass filter provide adequate protection for most applications. However, should some interfering frequency be particularly strong, special measures may have to be taken to suppress it. In such cases, a band-pass filter, which discriminates against all frequencies outside the pass band, will not be as efficient as one or more band-stop filters which discriminate against specific unwanted frequencies.

Band-stop filters can also separate one frequency from all others, for instance by using a 3-db hybrid feeding two band-stop filters, spaced so that the reflected signals add up in the fourth arm of the hybrid. The frequencies outside the stop band, which pass through the band-stop filters, may be recombined by a second hybrid, if so desired. In this manner a constant-resistance input impedance may be maintained at all frequencies, limited only by the hybrid bandwidth, while separating the frequency bands.

Generally, band-stop filters are concerned only with narrow frequency bands; the design formulas presented here are for such cases, with stop-band bandwidths up to a few per cent. The design formulas are presented with the figures, for convenient reference, and their derivation is given or indicated in the text. The realization of the lumped-constant resonant circuits with transmission-line elements is dealt with next. Formulas are given and a table is presented to facilitate numerical work. In the experimental lining-up procedure, each resonant branch is first adjusted to give the proper 3-db bandwidth, and formulas for this are given. The effects

of dissipation loss are then discussed. It is shown how the dissipation limits the maximum attenuation, the minimum reflection loss, and how it increases the insertion loss in the pass band.

A strip-transmission-line and a waveguide band-stop filter were constructed and tested. The experimental results were found to compare well with the performance predicted by the theory.

II. DERIVATION FROM LOW-PASS PROTOTYPE

The low-pass filter prototype[1,2] can be transformed by suitable frequency transformations into either a band-pass, a high-pass, or a band-stop filter. The transition from low-pass to band-stop characteristic can be effected by the transformation

$$\frac{1}{\omega'} = \frac{1}{w\omega_1'}\left(\frac{\omega}{\omega_0} - \frac{\omega_0}{\omega}\right) \tag{1}$$

where ω' stands for the radian frequency of the low-pass prototype filter and ω that of the band-stop filter. The remaining quantities in (1) are defined in Figs. 1 and 2.

It can be seen from (1) and Figs. 1 and 2 that frequencies in Table 1 correspond.

To obtain the L_i, C_i in Fig. 2 in terms of the g_i in Fig. 1, it is simpler (but not essential) to derive Fig. 2(a) from Fig. 1(a) and Fig. 2(b) from Fig. 1(b), so that series impedances go over to other series impedances, and shunt admittances to other shunt admittances. Multiplying both sides of (1) by $1/g_i$, one obtains the desired relation. For shunt branches, equating reactances,

$$\omega L_i - \frac{1}{\omega C_i} = \frac{1}{g_i\omega'} = \frac{1}{w\omega_1'g_i}\left(\frac{\omega}{\omega_0} - \frac{\omega_0}{\omega}\right) \tag{2}$$

which reduces to

$$\omega_0 L_i = \frac{1}{\omega_0 C_i} = \frac{1}{w\omega_1'g_i}. \tag{3}$$

For series branches, equating susceptances,

$$\omega C_j - \frac{1}{\omega L_j} = \frac{1}{g_j\omega'} = \frac{1}{w\omega_1'g_j}\left(\frac{\omega}{\omega_0} - \frac{\omega_0}{\omega}\right) \tag{4}$$

[1] S. B. Cohn, "Direct-coupled-resonator filters," PROC. IRE, vol. 45, pp. 187–196; February, 1957.
[2] G. L. Matthaei, *et al.*, Stanford Res. Inst., Menlo Park, Calif., SRI Project 2326, ch. 13; January, 1961.

which reduces to

$$\omega_0 C_j = \frac{1}{\omega_0 L_j} = \frac{1}{w\omega_1' g_j} \cdot \qquad (5)$$

The *reactance slope parameter* x of a reactance $X = \omega L - 1/\omega C$ is

$$x \equiv \frac{\omega_0}{2} \left. \frac{dX}{d\omega} \right|_{\omega=\omega_0} = \omega_0 L = 1/\omega_0 C, \qquad (6)$$

and similarly the *susceptance slope parameter* b of a susceptance $B = \omega C - 1/\omega L$ is

$$b \equiv \frac{\omega_0}{2} \left. \frac{dB}{d\omega} \right|_{\omega=\omega_0} = \omega_0 C = \omega_0 L. \qquad (7)$$

Now (3) for a shunt branch becomes

$$x_i = \frac{1}{w\omega_1' g_i} \qquad (8)$$

and (5) for a series branch becomes

$$b_j = \frac{1}{w\omega_1' g_j} \cdot \qquad (9)$$

The circuits shown in Fig. 2 have the same impedance levels as the prototypes in Fig. 1. To change to another impedance level, every R and every L should be multiplied by the impedance scale factor while every G and every C should be divided by it.
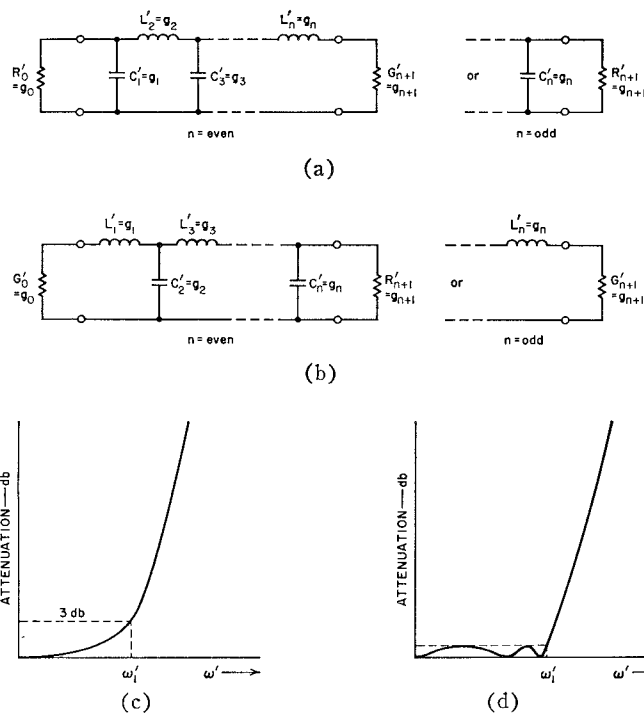

Fig. 1—Low-pass prototype filter. (a) and (b) Four basic circuit types, defining the parameters $g_0, g_1, \cdots, g_{n+1}$. (c) and (d) Maximally flat and equiripple characteristics, defining the band edge ω_1'.
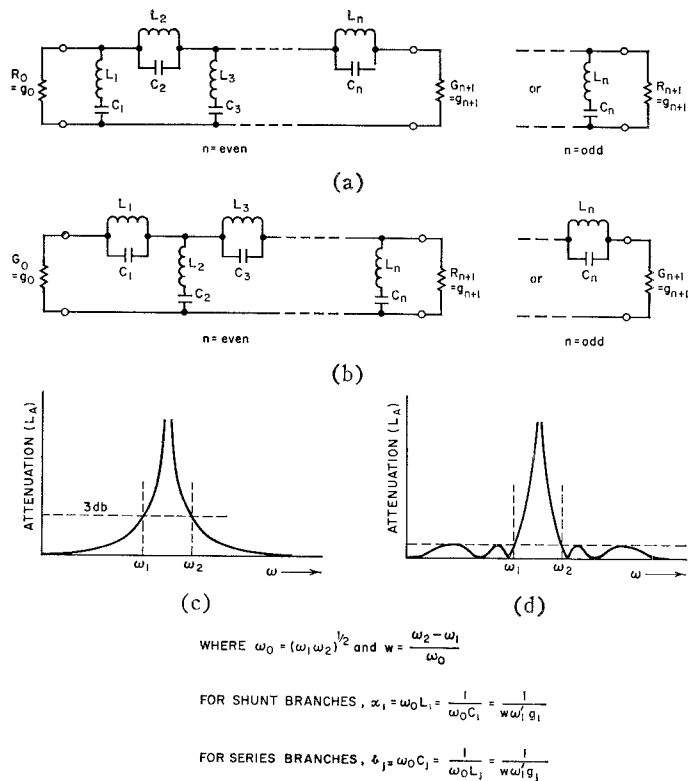

Fig. 2—Band-stop filter. (a) and (b) Four basic circuit types derivable from their four low-pass counterparts in Fig. 1. (c) and (d) Maximally flat and equiripple characteristics defining center frequency ω_0 and fractional bandwidth w.

WHERE $\omega_0 = (\omega_1\omega_2)^{1/2}$ and $w = \dfrac{\omega_2-\omega_1}{\omega_0}$

FOR SHUNT BRANCHES, $x_i = \omega_0 L_i = \dfrac{1}{\omega_0 C_i} = \dfrac{1}{w\omega_1' g_i}$

FOR SERIES BRANCHES, $b_j = \omega_0 C_j = \dfrac{1}{\omega_0 L_j} = \dfrac{1}{w\omega_1' g_j}$

TABLE I

RELATION BETWEEN VARIOUS FREQUENCIES IN THE PROTOTYPE- AND BAND-STOP FILTER RESPONSES

ω'	ω
0	0 or ∞
ω_1'	$\omega_{1,2} = \omega_0 \left[\left(1+\dfrac{w^2}{4}\right)^{1/2} \mp \dfrac{w}{2} \right]$
	$\approx \omega_0 \left(1 \mp \dfrac{w}{2}\right),$ when $w \ll 1$
∞	ω_0

$$\frac{x_1}{Z_0} = \frac{1}{\omega_1' g_0 g_1 w}$$

$$\left.\frac{x_1}{Z_0}\right|_{i=even} = \left(\frac{Z_1}{Z_0}\right)^2 \frac{g_0}{\omega_1' g_i w}$$

$$\left.\frac{x_1}{Z_0}\right|_{i=odd} = \frac{1}{\omega_1' g_0 g_i w}$$

$$\left(\frac{Z_1}{Z_0}\right)^2 = \frac{1}{g_0 g_{n+1}}$$

If $n = odd$, $Z_1 = Z_0$

(a)

$$\frac{x_1}{Z_0} = \frac{1}{\omega_1' g_0 g_1 w}$$

$$\left.\frac{x_1}{Z_0}\right|_{i=even} = \left(\frac{Z_1 \; Z_3}{Z_0 Z_2} \cdots \frac{Z_{i-1}}{Z_{i-2}}\right)^2 \frac{g_0}{\omega_1' g_i w}$$

$$\left.\frac{x_1}{Z_0}\right|_{\substack{i=odd \\ i\neq 1}} = \left(\frac{Z_2 Z_4}{Z_1 Z_3} \cdots \frac{Z_{i-1}}{Z_{i-2}}\right)^2 \frac{1}{\omega_1' g_0 g_i w}$$

If $n = even$, $\dfrac{Z_0}{Z_n} = \left(\dfrac{Z_0 Z_2}{Z_1 Z_3} \cdots \dfrac{Z_{n-2}}{Z_{n-1}}\right)^2 \dfrac{1}{g_0 g_{n+1}}$, or

If $n = odd$, $\dfrac{Z_0}{Z_n} = \left(\dfrac{Z_1 Z_3}{Z_2 Z_4} \cdots \dfrac{Z_{n-2}}{Z_{n-1}}\right)^2 \dfrac{g_0}{g_{n+1}}$
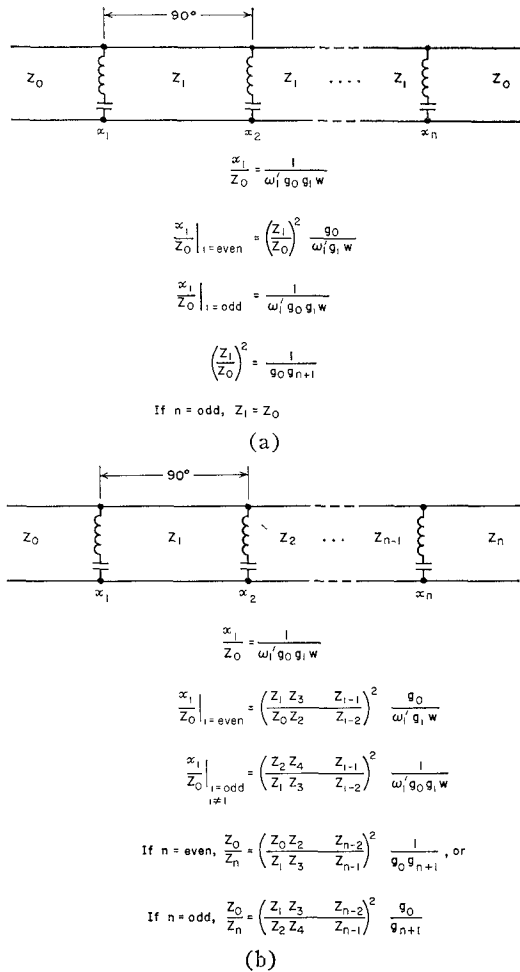
(b)

Fig. 3—Band-stop filter with shunt branches and quarter-wave couplings (a) Equal inverter impedances Z_1. (b) General case of unequal inverter impedances.

$$\frac{\ell_1}{Y_0} = \frac{1}{\omega_1' g_0 g_1 w}$$

$$\left.\frac{\ell_1}{Y_0}\right|_{i=even} = \left(\frac{Y_1}{Y_0}\right)^2 \frac{g_0}{\omega_1' g_i w}$$

$$\left.\frac{\ell_1}{Y_0}\right|_{i=odd} = \frac{1}{\omega_1' g_0 g_i w}$$

If $n = even$, $\left(\dfrac{Y_1}{Y_0}\right)^2 = \dfrac{1}{g_0 g_{n+1}}$

If $n = odd$, $Y_1 = Y_0$

(a)

$$\frac{\ell_1}{Y_0} = \frac{1}{\omega_1' g_0 g_1 w}$$

$$\left.\frac{\ell_1}{Y_0}\right|_{i=even} = \left(\frac{Y_1 \; Y_3}{Y_0 Y_2} \cdots \frac{Y_{i-1}}{Y_{i-2}}\right)^2 \frac{g_0}{\omega_1' g_i w}$$

$$\left.\frac{\ell_1}{Y_0}\right|_{\substack{i=odd \\ i\neq 1}} = \left(\frac{Y_2 Y_4}{Y_1 Y_3} \cdots \frac{Y_{i-1}}{Y_{i-2}}\right)^2 \frac{1}{\omega_1' g_0 g_i w}$$

If $n = even$, $\dfrac{Y_0}{Y_n} = \left(\dfrac{Y_0 Y_2}{Y_1 Y_3} \cdots \dfrac{Y_{n-2}}{Y_{n-1}}\right)^2 \dfrac{1}{g_0 g_{n+1}}$, or

If $n = odd$, $\dfrac{Y_0}{Y_n} = \left(\dfrac{Y_1 Y_3}{Y_2 Y_4} \cdots \dfrac{Y_{n-2}}{Y_{n-1}}\right)^2 \dfrac{g_0}{g_{n+1}}$
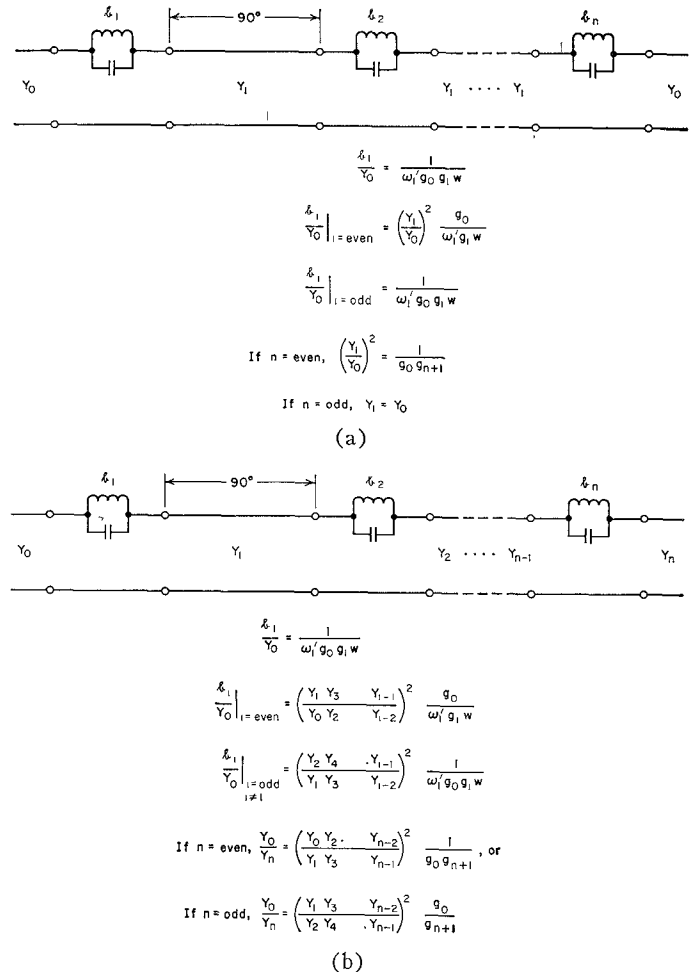
(b)

Fig. 4—Band-stop filter with series branches and quarter-wave couplings. (a) Equal inverter admittances, Y_1. (b) General case of unequal inverter admittances.

To realize a band-stop filter in transmission line, it is more convenient to use only shunt branches, or only series branches. The circuit of Fig. 2(a) can be converted into a circuit with only series-resonant shunt branches by means of impedance inverters, which take the form of (frequency-invariant) 90° line lengths, as shown in Fig. 3. The reactance slope parameters of this circuit in terms of the low-pass prototype parameters $g_0, g_1, \cdots$, g_{n+1} are also given in Fig. 3. These formulas can be deduced with the help of Figs. 1 and 2, and the impedance-inverting property of quarter-wave lines.

In the circuit of Fig. 3(a), the output impedance and the input impedance have both been set equal to Z_0. In the case of maximally-flat filters, or Chebyshev filters with n odd, the whole line of impedance inverters can be uniform, with the 90° lines all having impedances $Z_1 = Z_0$. However, for Chebyshev filters with n even, the low-pass prototype is not symmetrical, and the simplest way to obtain a symmetrical band-stop filter of the type shown in Fig. 3(a) is to set the impedances of all the 90° lines equal to Z_1, which ceases to be equal to Z_0, and is given by

$$\left(\frac{Z_1}{Z_0}\right)^2 = \frac{1}{g_0 g_{n+1}} \qquad (10)$$

as stated in Fig. 3(a).

If the slope parameters determined by Fig. 3(a) are either too small or too large to realize conveniently, they may be adjusted up or down by controlling the impedances of the 90° lines. The formulas for the general case are given in Fig. 3(b). They reduce to the case of Fig. 3(a) when $Z_1 = Z_2 = \cdots = Z_{n-1}$. It should be noted that if the Z_i are chosen unequal, then greater reflections will generally result somewhere in the pass band than would occur with a uniform impedance level $Z_i = Z_0$.

The dual of the band-stop filter with only shunt branches (Fig. 3) is the band-stop filter with only series branches, shown in Fig. 4. It can be derived from the circuit of Fig. 2(b), and may be regarded as the dual of the circuit of Fig. 3.

III. Realization of Resonant Circuits in Transmission Line

In strip transmission line or coaxial line, the circuit of Fig. 3 may be realized by using noncontacting stubs, as shown in Fig. 5, with the gaps forming the capacitances required in Fig. 3, and the stubs approximating the inductances. The stubs may be short-circuited and just under 90° long, as shown in Fig. 5 and indicated in

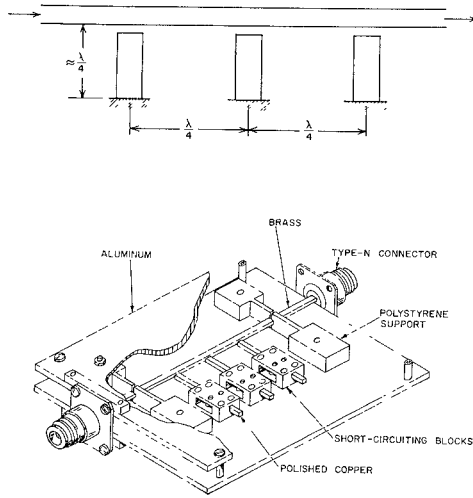Fig. 5—Strip-transmission-line band-stop filter (a) Schematic. (b) Sketch of actual filter with three stubs.

WHERE $F(\phi) = \phi \sec^2 \phi + \tan \phi$ (TABLE 2)

$G(\phi) = 2 F(\phi) + \frac{1}{\pi}(2\delta - \sin 2\delta)$
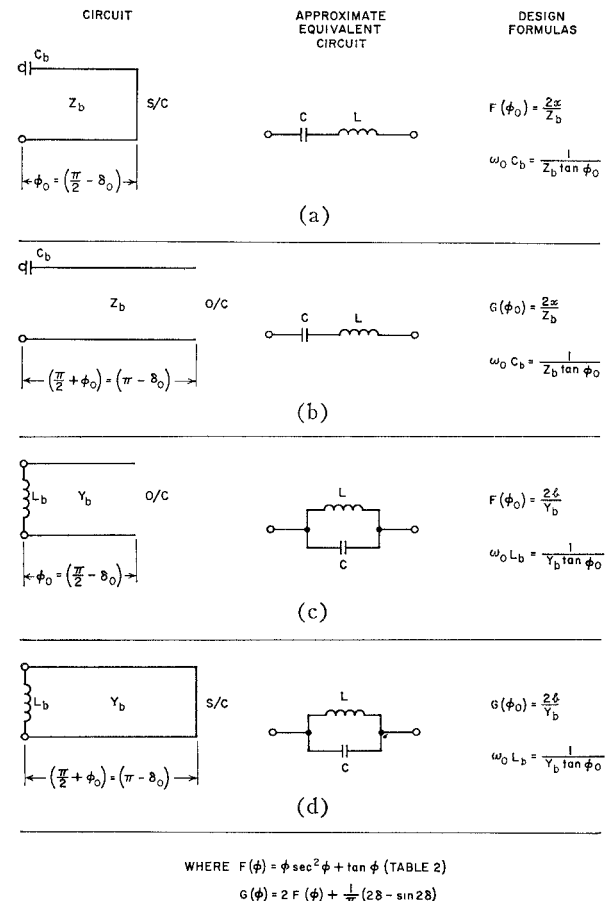
Fig. 6—Realization of resonant circuits in transmission line. (a) and (b) Series resonant circuit suitable for strip or coaxial line (Fig. 5). (c) and (d) Shunt resonant circuit suitable for waveguide.

Fig. 6(a); or they may be open-circuited and just under 180° long, as indicated in Fig. 6(b). The frequency dependence of the stub reactance of Fig. 6(a) is not the same as that of a lumped-constant inductance; the two stub parameters {characteristic impedance Z_b, and electrical length $\phi = [(\pi/2) - \delta]$ radians} must be chosen to give the same reactance slope parameter as in (6) to obtain the same response near resonance. The condition for this will now be derived, and the three remaining cases of Fig. 6(b), (c) and (d) may then be treated as an extension of the first case.

The transmission lines will be supposed to be nondispersive. (If waveguide or other dispersive line is used, replace normalized frequency ω/ω_0 by normalized reciprocal guide wavelength λ_{g0}/λ_g, where λ_g and λ_{g0} are the guide wavelengths at frequencies ω and ω_0, respectively.) Applying the resonant condition when $\omega = \omega_0$ and $\phi = \phi_0$,

$$Z_b \tan \phi_0 = \frac{1}{\omega_0 C_b} \qquad (11)$$

and since ϕ is proportional to ω,

$$\frac{d\phi}{\phi} = \frac{d\omega}{\omega}. \qquad (12)$$

The following determine the reactance slope parameter:

$$x = \frac{\omega_0}{2} \frac{d}{d\omega}\left(Z_b \tan \phi - \frac{1}{\omega C}\right)\bigg|_{\omega=\omega_0, \phi=\phi_0}, \qquad (13)$$

$$= \frac{Z_b}{2}\left(\phi_0 \sec^2 \phi_0 + \tan \phi_0\right) = \frac{Z_b}{2} F(\phi_0) \qquad (14)$$

where the function $F(\phi)$ is defined by

$$F(\phi) = \phi \sec^2 \phi + \tan \phi. \qquad (15)$$

This function can be determined numerically from Table II (next page).

To determine the three parameters C_b, Z_b, and ϕ_0, one of them may be selected arbitrarily, for instance Z_b. The slope parameter x is determined from Fig. 3 or 4. For the circuit of Fig. 6(a), ϕ_0 is determined from the assumed value for Z_b by use of (14) and Table II; and finally (11) yields C_b. These formulas and the ones corresponding to all four cases are summarized in Fig. 6.

For a given ϕ_0 and Z_b or Y_b, the slope parameter of the near-180° line is almost twice as great as the slope parameter of the near-90° line. More precisely, for the near-180° lines [Cases (b) and (d) in Fig. 6] one has to substitute

$$G(\phi) = \left(\frac{\pi}{2} + \phi\right)\sec^2 \phi + \tan \phi \qquad (16)$$

(ϕ in radians) for $F(\phi)$, which was used with the near-90° lines [Cases (a) and (c) in Fig. 6]. This can be written more conveniently as

$$G(\phi) = 2F(\phi) + \frac{2\delta - \sin 2\delta}{\pi} \qquad (17)$$

where

$$\delta = \frac{\pi}{2} - \phi \qquad (18)$$

TABLE II

TABLE* OF $F(\phi) = \phi \sec^2 \phi + \tan \phi$

$\phi°$	$F(\phi)$	$\phi°$	$F(\phi)$	$\phi°$	$F(\phi)$	$\phi°$	$F(\phi)$	$\phi°$	$F(\phi)$	$\phi°$	$F(\phi)$
89.80	128907.01	83.80	134.59	77.80	35.03	71.80	15.88	65.80	9.05	59.00	5.54
89.60	32227.14	83.60	126.34	77.60	33.92	71.60	15.54	65.60	8.91	59.00	5.20
89.40	14324.32	83.40	118.82	77.40	32.86	71.40	15.22	65.40	8.77	57.00	4.89
89.20	8057.53	83.20	111.96	77.20	31.85	71.20	14.90	65.20	8.63	56.00	4.60
89.00	5157.05	83.00	105.68	77.00	30.88	71.00	14.59	65.00	8.49	55.00	4.34
88.80	3581.46	82.80	99.91	76.80	29.96	70.80	14.29	64.80	8.36	54.00	4.10
88.60	2631.38	82.60	94.60	76.60	29.09	70.60	14.00	64.60	8.23	53.00	3.88
88.40	2014.78	82.40	89.71	76.40	28.24	70.40	13.72	64.40	8.10	52.00	3.67
88.20	1592.03	82.20	85.19	76.20	27.44	70.20	13.45	64.20	7.98	51.00	3.48
88.00	1289.64	82.00	81.00	76.00	26.67	70.00	13.19	64.00	7.86	50.00	3.30
87.80	1065.91	81.80	77.11	75.80	25.93	69.80	12.93	63.80	7.74	49.00	3.13
87.60	895.73	81.60	73.50	75.60	25.22	69.60	12.68	63.60	7.62	48.00	2.98
87.40	763.30	81.40	70.14	75.40	24.55	69.40	12.44	63.40	7.51	47.00	2.83
87.20	658.21	81.20	67.01	75.20	23.89	69.20	12.21	63.20	7.40	46.00	2.69
87.00	573.44	81.00	64.08	75.00	23.27	69.00	11.98	63.00	7.29	45.00	2.57
86.80	504.05	80.80	61.34	74.80	22.67	68.80	11.76	62.80	7.19	44.00	2.44
86.60	446.55	80.60	58.77	74.60	22.09	68.60	11.54	62.60	7.08	43.00	2.33
86.40	398.36	80.40	56.36	74.40	21.53	68.40	11.33	62.40	6.98	42.00	2.22
86.20	357.58	80.20	54.10	74.20	21.00	68.20	11.13	62.20	6.88	41.00	2.12
86.00	322.76	80.00	51.97	74.00	20.48	68.00	10.93	62.00	6.79	40.00	2.02
85.80	292.79	79.80	49.97	73.80	19.99	67.80	10.73	61.80	6.69	39.00	1.93
85.60	266.82	79.60	48.08	73.60	19.51	67.60	10.55	61.60	6.60	38.00	1.84
85.40	244.16	79.40	46.29	73.40	19.05	67.40	10.36	61.40	6.51	37.00	1.76
85.20	224.27	79.20	44.61	73.20	18.60	67.20	10.18	61.20	6.42	36.00	1.68
85.00	206.73	79.00	43.01	73.00	18.17	67.00	10.01	61.00	6.33	35.00	1.61
84.80	191.16	78.80	41.50	72.80	17.76	66.80	9.84	60.80	6.24	34.00	1.53
84.60	177.29	78.60	40.07	72.60	17.36	66.60	9.68	60.60	6.16	33.00	1.46
84.40	164.89	78.40	38.71	72.40	16.97	66.40	9.51	60.40	6.08	32.00	1.40
84.20	153.74	78.20	37.42	72.20	16.59	66.20	9.36	60.20	6.00	31.00	1.33
84.00	143.69	78.00	36.19	72.00	16.23	66.00	9.20	60.00	5.92	30.00	1.27

* Note: $F(\phi) \approx (1/2)G(\phi)$.

is the amount by which the line length falls short of $\pi/2$ or π radians, respectively. The last term in (17), namely, $(2\delta - \sin 2\delta)/\pi$, is usually very small, so that $G(\phi)$ is very nearly twice $F(\phi)$. For instance, when $\phi = \pi/3 = 60°$, the error in $G(\phi)$ due to neglecting this term in (17) is less than one-half per cent, while for $\phi = \pi/4 = 45°$, the error is 3.4 per cent. One may therefore still use Table II to solve for ϕ_0, looking up $F(\phi) \approx (1/2)G(\phi)$, and subsequently making a small correction if ϕ_0 is smaller than about 60° or 45°.

IV. FRACTIONAL 3-DB BANDWIDTH OF A SINGLE BRANCH

The impedance Z_b and length at resonance ϕ_0, of the stub can generally be translated more or less accurately into physical dimensions, but the capacitance C_b or inductance L_b can be constructed only approximately. Some individual adjustment of each branch circuit is desirable to provide the proper slope parameter. The adjustment may be provided in strip or coaxial line by sliding the stub to alter the capacitive gap (Fig. 5). The other stubs are removed or detuned, while each stub in turn is adjusted for the desired slope parameter. This is experimentally determined when each stub alone has the proper stop-band bandwidth. The 3-db fractional bandwidths of the four cases considered are given in Fig. 7. Case (a) in Fig. 7 may for instance be derived by noting that the insertion loss of a reactance X in

shunt across a line of impedance Z_1 is 3 db when the reactance has the value $X = (1/2)Z_1$. By (14)

$$\frac{Z_b}{2}F(\phi_0) = x = \frac{\omega_0}{2}\frac{dX}{d\omega}\bigg|_{\omega=\omega_0}. \tag{19}$$

Since we are only considering small bandwidths, we may replace $2d\omega/\omega_0$ by the 3-db bandwidth, u, and dX by $(1/2)Z_1$. Then

$$u = \frac{Z_1}{Z_b}\frac{1}{F(\phi_0)}. \tag{20}$$

The formulas presented in Fig. 7 are similarly derived. They are more general in that they consider the case of a reactance X shunting the junction of two lines of different impedances Z_0 and Z_1 [Fig. 7(a) and (b)], as well as the dual series case [Fig. 7(c) and (d)]. This more general case (when Z_0 is not equal to Z_1) is of interest mainly for the first and last branches of Chebyshev filters with n even [Figs. 3(a) and 4(a)]. In most cases Z_0 will be equal to Z_1, and the factor $h(r)$ in Fig. 7 will then be unity; the first formula in Fig. 7, for instance, will reduce to (20).

We may note in passing that if $r = Z_1/Z_0$ or Y_1/Y_0 is greater than $3 + 2\sqrt{2} = 5.8284$ or less than $3 - 2\sqrt{2} = 0.1716$, then the 3-db bandwidth does not exist, since the intrinsic mismatch of the junction causes a 3-db reflection loss and any reactance at the junction can only
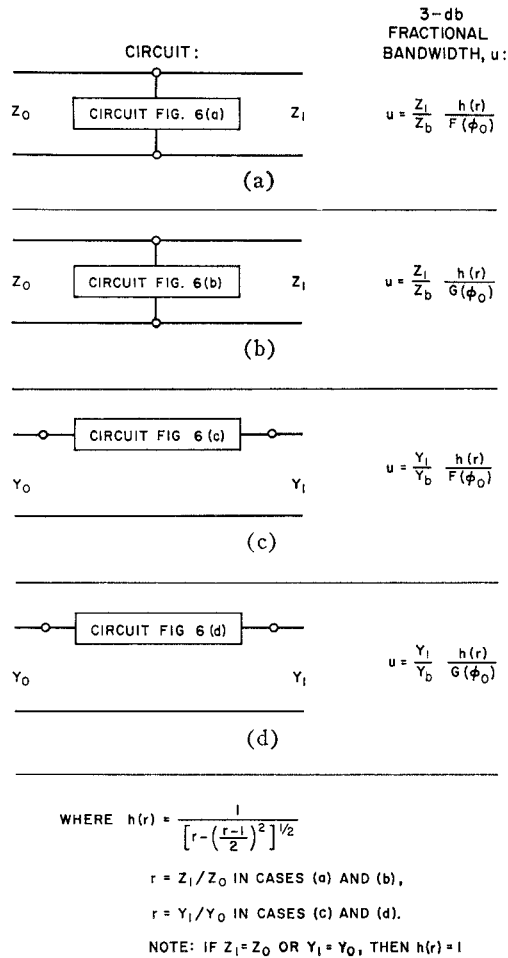
CIRCUIT:	3-db FRACTIONAL BANDWIDTH, u:

Z_0 — CIRCUIT FIG. 6(a) — Z_1 $u = \dfrac{Z_1}{Z_b}\,\dfrac{h(r)}{F(\phi_0)}$

(a)

Z_0 — CIRCUIT FIG. 6(b) — Z_1 $u = \dfrac{Z_1}{Z_b}\,\dfrac{h(r)}{G(\phi_0)}$

(b)

CIRCUIT FIG 6(c) $u = \dfrac{Y_1}{Y_b}\,\dfrac{h(r)}{F(\phi_0)}$
Y_0 Y_1

(c)

CIRCUIT FIG 6(d) $u = \dfrac{Y_1}{Y_b}\,\dfrac{h(r)}{G(\phi_0)}$
Y_0 Y_1

(d)

WHERE $h(r) = \dfrac{1}{\left[r-\left(\frac{r-1}{2}\right)^2\right]^{1/2}}$

$r = Z_1/Z_0$ IN CASES (a) AND (b),

$r = Y_1/Y_0$ IN CASES (c) AND (d).

NOTE: IF $Z_1 = Z_0$ OR $Y_1 = Y_0$, THEN $h(r) = 1$

Fig. 7—3-db fractional bandwidth of single stubs across the junction of two transmission lines.

serve to increase it. A 10-db or similar bandwidth would then have to be used for the experimental adjustment. However, such cases are not likely to arise in practice and will not be considered further.

V. Effect of Dissipation Loss

The following effects of dissipation loss (finite unloaded Q) are recognized:

1) The peak attenuation inside the stop band is not infinite, but remains limited.

2) The reflection coefficient does not reach unity anywhere inside the stop band, resulting in an imperfect short circuit, and loss of power on reflection.

3) There is additional loss in the pass band of the filter.

These three effects will now be considered in turn.

A. Peak Attenuation

We introduce resistances into the first circuit of Fig. 2(a) to allow for dissipation. At resonance the reactive elements cancel and only the resistances remain. In Fig. 8, G_1 is the conductance in the first resonant circuit, R_2 is the resistance in the second resonant circuit, etc. If

(1) MAXIMUM ATTENUATION

$L_{A\,(max)} \approx 20\,\Sigma_{i=1}^{n}\log_{10}(q_i D_i) + 10\,\log_{10}\left(\dfrac{q_0\,q_{n+1}}{4}\right)$ db

WHERE $D_i = w\omega_i' Q_{ui}$

(2) MINIMUM RETURN LOSS·

$\approx \dfrac{1737}{w\omega_1' q_0 q_1 Q_{u1}}$ db

(3) PASS-BAND DISSIPATION LOSS:

$L_d \approx 1.086\, w\omega_1'\left(\dfrac{\omega_0}{\omega-\omega_0}\right)^2\left[\dfrac{q_1 q_0}{Q_{u1}} + \dfrac{q_2/q_0}{Q_{u2}} + \dfrac{q_3 q_0}{Q_{u3}} + \dfrac{q_4/q_0}{Q_{u4}} + \cdots\right]$

Fig. 8—Effect of dissipation.

Q_{ui} is the unloaded Q of the ith resonator, then by Fig. 2,

$$G_1 = \frac{Q_{u1}}{x_1} = w\omega_1' g_1 Q_{u1}$$
$$R_2 = \frac{Q_{u2}}{b_2} = w\omega_1' g_2 Q_{u2} \qquad (21)$$
$$\text{etc.}$$

If the Q_{ui} are large enough, then any R_i or $1/G_i$ ($i=1$, $2, \cdots, n$) is much less than both R_0 and $1/G_{n+1}$. The output voltage V (Fig. 8) is then given by

$$\frac{V}{E} = \left(\frac{1}{R_0 G_1}\right)\left(\frac{1}{R_2 G_3}\right)\cdots\left(\frac{1}{R_n G_{n+1}}\right). \qquad (22)$$

Since the available power is $E^2/4R_0$, while the power absorbed in the load is $V^2 G_{n+1}$, the insertion loss L_A is given by their ratio,

$$L_A = 10\log\frac{E^2}{4R_0}\cdot\frac{1}{V^2 G_{n+1}}$$
$$= 10\log\frac{(R_0 G_1 R_2 G_3 \cdots R_n G_{n+1})^2}{4R_0 G_{n+1}}. \qquad (23)$$

The first formula given in Fig. 8 can now be deduced from (21) and (23). This formula has been proved only for the circuit in Fig. 8, which corresponds to the first circuit in Fig. 2(a); however, its final form stated in Fig. 8 is general, and holds for all four circuits in Fig. 2.

B. Minimum-Return Loss

The peak reflection is determined almost completely by the dissipation in the first resonator (nearest the generator). At resonance the VSWR is $R_0 G_1$ (Fig. 8), which is given by (21) in terms of Q_{u1}. If the reflection coefficient is denoted by Γ, the return loss is $(1-|\Gamma|^2)$. This leads to the general minimum-return loss formula in Fig. 8, which applies when Q_{u1} is large. It is stated in decibels in Fig. 8.

C. Dissipation Loss in Pass Band Near Stop Band

In the pass band immediately above dc, the shunt branch reactances X_1, X_3, $\cdots$ (Fig. 8) are high com-

pared to the resistances $1/G_1$, $1/G_3$, $\cdots$ in series with them, and both are small (for large enough Q) compared to the load and source impedances, R_0 and $1/G_{n+1}$. Similarly, the series branch impedances $1/B_2$, $1/B_4$, $\cdots$ are then small compared to the resistances R_2, R_4, $\cdots$ in shunt with them, and both are small compared to R_0 and $1/G_{n+1}$.

Under these conditions, the respective total currents in the shunt branches are determined largely by the reactances X_1, X_3, $\cdots$, and are approximately equal to $E/2X_1$, $E/2X_3$, etc.; similarly, the respective total voltage drops across the series branches are approximately equal to $E/(2R_0B_2)$, $E/(2R_0B_4)$, etc. The power dissipated in the first shunt branch is then approximately equal to $(E/2X_1)^2/G_1$, and in the first series branch it is $(E/2R_0B_2)^2/R_2$. The available power is $E^2/4R_0$. The (small) dissipation loss, L_d, is then proportional to the ratio of the sum of all the former to the latter, and is

$$L_d = \frac{4.343}{R_0} \left[\frac{1}{G_1 X_1^2} + \frac{1}{R_2(R_0 B_2)^2} + \cdots \right] db. \quad (24)$$

The pass-band region near the stop band will generally be of more interest than the region near dc. Eq. (24) will become less accurate near the stop band, as the branches approach resonance, and may then be expected to provide a lower bound to the dissipation loss. At a frequency $\omega = \omega_0 + \Delta\omega$ near the stop band, X_1, B_2, etc. are given by

$$\left. \begin{aligned} X_1 &\approx 2x_1 \frac{\Delta\omega}{\omega_0} \\ B_2 &\approx 2b_2 \frac{\Delta\omega}{\omega_2} \\ \text{etc.} \end{aligned} \right\} \quad (25)$$

Using (21) and the formulas in Fig. 2, one finally reduces L_d to the expression given in Fig. 8, which is general and which holds for all four circuit forms of Fig. 2 with losses added. (The g_i with odd i appear in normalized form $g_i g_0$, while the g_i with even i appear in normalized form g_i/g_0.) The expression for L_d in Fig. 8 will generally be of the right order of magnitude; however, the actual dissipation loss near band edge may be expected to be several times the value of L_d predicted from Fig. 8.

VI. Example of Strip-Line Design

A band-stop filter is required with the following specifications:

Frequency of infinite attenuation, f_0: 4.0 Gc.
Pass-band ripple: 0.5 db.
Stop-band bandwidth to equiripple (0.5-db) points: 5 per cent.
Minimum attenuation over 2 per cent stop band: 20 db.

It is necessary to determine the number of branches. This is accomplished by substituting ω'/ω_1' from (1),

$$\frac{\omega'}{\omega_1'} = \frac{\omega}{\dfrac{\omega}{\omega_0} - \dfrac{\omega_0}{\omega}} = 2.5 \quad (26a)$$

into the expression

$$L_A = 10 \log_{10} \left[1 + (10^{L_{Am}/10} - 1) \right.$$
$$\left. \cdot \cosh^2 \left(n \cosh^{-1} \frac{\omega'}{\omega_1'} \right) \right] db. \quad (26b)$$

which is the last equation of Fig. 2,[1] where L_{Am} is the pass-band ripple in decibels, and ω_1' is the cutoff frequency. In this case $L_{Am} = 0.5$ and $\omega'/\omega_1' = 2.5$. A two-branch filter gives only 12.3-db attenuation, while a three-branch filter gives 25.8 db. Therefore the number of branches, n, must be at least three, to give more than 20-db attenuation over a 2 per cent stop band. Hence we choose $n = 3$.

The low-pass prototype parameters for 0.5-db ripple and $n = 3$ are[2]

$$g_0 = g_4 = 1.0$$
$$g_1 = g_3 = 1.5963 \quad (27)$$
$$g_2 = 1.0967$$

and $\omega' = 1$. The filter takes the form shown in Fig. 5. From Fig. 3,

$$\left. \begin{aligned} \frac{x_1}{Z_0} &= \frac{x_3}{Z_0} = 12.528 \\ \frac{x_2}{Z_0} &= 18.232 \end{aligned} \right\} \quad (28)$$

The characteristic impedance of the main line, Z_0, was made 50 ohms, and consisted of a solid strip conductor 0.184 inch wide and 0.125 inch high, with a plate-to-plate spacing of 0.312 inch. The branch stubs were each made of square cross section, 0.125 inch by 0.125 inch, which gives the impedances[3] $Z_{b1} = Z_{b2} = Z_{b3} = 59.4$ ohms [see Fig. 5(b)]. Therefore from Fig. 6, circuit (a),

$$F(\phi_{01}) = F(\phi_{03}) = \frac{2x_1}{Z_0} \cdot \frac{Z_0}{Z_{b_1}} = 21.1 \left. \right\}$$

and

$$F(\phi_{02}) = \frac{2x_2}{Z_0} \cdot \frac{Z_0}{Z_{b_2}} = 30.7 \left. \right\} \quad (29)$$

[3] R. H. T. Bates, "The characteristic impedance of the shielded slab line," IRE TRANS. ON MICROWAVE THEORY AND TECHNIQUES, vol. MTT-4, pp. 28–33; January, 1956.

which can be solved by Table II,

$$\phi_{01} = \phi_{03} = 74.2° = 1.295 \text{ radians}$$
$$\phi_{02} = 77.0° = 1.344 \text{ radians}$$

(30)

Again from Fig. 6, we obtain

$$\omega_0 C_{b_1} = \omega_0 C_{b_3} = 0.004764 \text{ mho}$$
$$\omega_0 C_{b_2} = 0.003888 \text{ mho}$$

(31)

which at 4.0 Gc yields

$$C_{b_1} = C_{b_3} = 0.1893 \text{ pf}$$
$$C_{b_2} = 0.1546 \text{ pf}$$

(32)

With 0.125-by-0.125-inch stubs, such capacitances are obtained with a gap in the order of 0.031 inch, which is a quite suitable value, being small compared to a wavelength but still large enough to be achieved accurately without special precautions (like dielectric spacers, which would increase the dissipation loss).

The length of the stubs is determined by (30) and the wavelength, which is 2.950 inches at 4.0 Gc. It was at first assumed that the reference plane was in the face opposite the main line. The capacitive gap of each stub was adjusted to give peak attenuation at 4.0 Gc and the width of the stop band was then measured. The 3-db fractional bandwidths u_i are given by Fig. 6,

$$u_1 = u_3 = \frac{Z_0}{Z_{b_1}} \frac{1}{F(\phi_{01})} = 4.00 \text{ per cent}$$
$$u_2 = \frac{Z_0}{Z_{b_2}} \frac{1}{F(\phi_{02})} = 2.74 \text{ per cent}$$

(33)

At first, the measured bandwidths were slightly too narrow, showing the coupling to be too loose and the stubs to be too long. The reference planes were thus not in the face opposite the main line, as was assumed for a first approximation, but were about two or three thousandths of an inch out in front. The stubs were accordingly shortened slightly to the following final dimensions: outer stub length 0.605 inch, gap 0.0305 inch; middle stub length 0.629 inch, gap 0.045 inch. All these stubs were then placed along the line as shown in Fig. 5. They are nominally 90° apart between reference planes at 4.0 Gc, but the spacing is not critical and they were simply placed a quarter-wavelength apart between centers (0.738 inch) and not further adjusted.

It is important that there should be no interaction, or mutual coupling, between stubs: with a ground-plane spacing of 0.3125 inch, the attenuation of the TE_{10} mode (electric vector parallel to the ground planes) from stub to stub is more than 50 db at 4.0 Gc, which should be adequate; it is also necessary to maintain proper centering so as not to excite the parallel-plate mode.

The response of this filter was computed on a digital computer and is plotted in Fig. 9. The points shown are the measured results on the experimental filter. The white circles represent the measured reflection loss of the
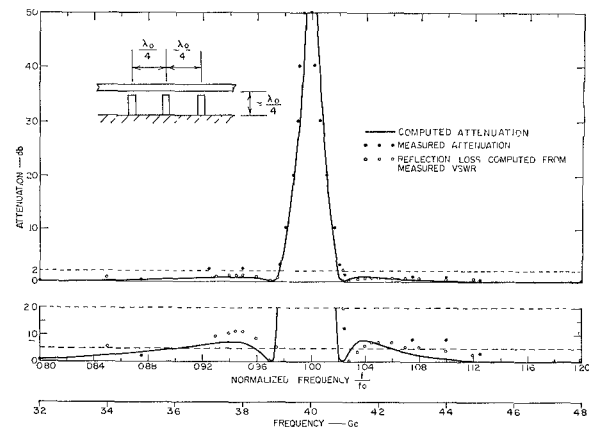

Fig. 9—Computed and measured response of a strip-line band-stop filter with $\lambda_0/4$ spacings between resonators.

filter, which may be compared with the computed curve, while the black circles represent the total measured insertion loss, including the effect of dissipation. The computed reflection loss reaches a ripple height of 0.7 db below, and 0.8 db above 4.0 Gc (instead of 0.5 db, which was the design goal). The measured reflection loss reaches a peak of 1.2 db below, and 0.7 db above 4.0 Gc.

The peak attenuation of the three-resonator filter was too great to measure, but the peak attenuation of each branch separately was measured. This gave 32 db for each of the two outer branches, and 28 db for the middle branch alone. Working back from Fig. 8, this leads to unloaded Q values of 1000. The theoretical unloaded Q of such a pure all-copper line at this frequency is 2600. In this case the strip conductors of the resonators were made of polished copper from commercial stock and the ground planes were aluminum. Other losses were presumably introduced by the current concentrations caused by fringing fields at the gap, and by the short-circuit clamps. The value of $Q_u = 1000$ is consistent with experimental results generally obtained. The peak attenuation of all three branches together should by the first formula of Fig. 8 reach a value of 104 db, which however, was beyond the measurement range of the available test equipment.

According to the formula for the dissipation loss L_d in Fig. 8, the dissipation loss should be only 0.04 db at 0.9 or 1.1 times the stop-band center frequency. The measured dissipation loss within this frequency interval was found to be several times the value predicted by the formula for L_d in Fig. 8, as is to be expected.

The bandwidth of the stop band to the 0.5-db points, both measured and computed, is 5.0 per cent, which is exactly the design goal. The attenuation over a 2 per cent band exceeds 25.4 db by computation. (Compare the 20-db design specification, and the 25.8 db predicted for a three-branch filter.) The measured points in the stop band also fall on the computed curve (Fig. 9).

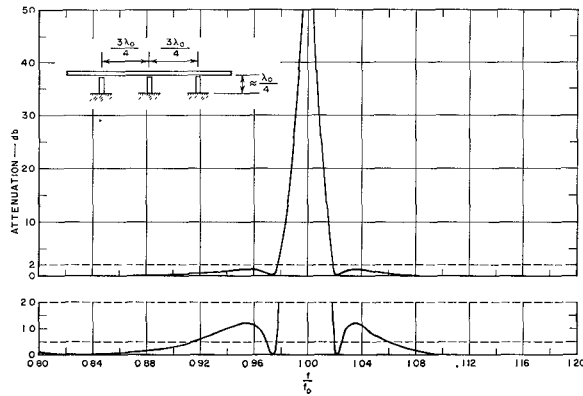In this case the interaction between resonators was negligible, making one-quarter-wave separations possi-

Fig. 10—Computed response of a strip-line filter
having $3\lambda_0/4$ spacings between resonators.

Fig. 11—Waveguide realization of band-stop filter.

ble. It is of interest to compare the performance of a band-stop filter with three-quarter-wave spacings, which might be required at higher frequencies for the same strip transmission line dimensions to let the evanescent modes between resonators be attenuated sufficiently. The performance of such a filter is shown in Fig. 10. A slight narrowing in the bandwidth of the stop band is observed, and the ripple height increases, but generally the performance is not affected greatly.

VII. WAVEGUIDE BAND-STOP FILTER CONSIDERATIONS

A waveguide band-stop filter is most conveniently realized using only series elements spaced an odd multiple of a quarter wavelength apart along the waveguide. The equivalent circuit of such a filter is shown in Fig. 4, while Fig. 11 shows a sketch of a waveguide realization of the filter. It is seen that the resonators in Fig. 11 are spaced at intervals of three-quarters of a guide wavelength.

Placing the resonators at one-quarter guide-wavelength intervals is not practical, because strong interaction results between the resonators by way of the fields about the coupling apertures. This interaction in an experimental band-stop filter, with quarter-guide-wavelength-spaced resonators, caused the stop-band response to have three peaks of high attenuation, with relatively low attenuation valleys in between, instead of the single high attenuation peak that is desired. (See Section VIII.)

As explained in Section III, the appropriate normalized frequency variable to use with dispersive lines, as in a waveguide filter, is the normalized reciprocal guide wavelength, λ_{g0}/λ_g. Thus, a waveguide filter and a strip-line filter, each designed from the same low-pass prototype and each having the same fractional bandwidth w, will have identical responses if the waveguide filter response is plotted on a λ_{g0}/λ_g scale and the strip-line filter response on a ω/ω_0 scale. On this basis, the formula, which for the strip-line filter was

$$w = \frac{\omega_2 - \omega_1}{\omega_0} = \frac{\omega_2}{\omega_0} - \frac{\omega_1}{\omega_0} \quad \text{(TEM mode)} \quad (34)$$
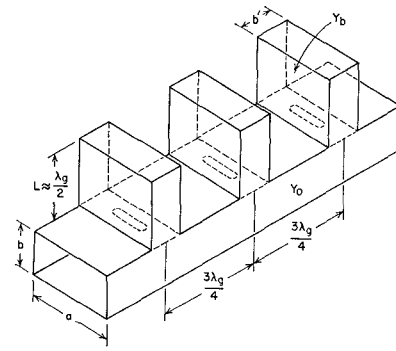
where ω_0, ω_1, and ω_2 are as defined in Fig. 2, is now replaced for a waveguide filter by

$$w = \frac{\lambda_{g0}}{\lambda_{g2}} - \frac{\lambda_{g0}}{\lambda_{g1}} \quad \text{(waveguide)} \quad (35)$$

where λ_{g0}, λ_{g1}, and λ_{g2} are analogously defined as the guide wavelengths at mid-stop band, and at the lower and upper edges of the stop band on a reciprocal guide-wavelength scale. If both responses are plotted on a frequency scale, however, the response of the waveguide filter derived from the same prototype will be considerably narrower. For small stop-band bandwidths, the fractional width of the stop band on a frequency scale will be approximately $(\lambda_0/\lambda_{g0})^2$ times w, which is the fractional bandwidth on a reciprocal guide-wavelength scale given by (35). (λ_0 is the free-space wavelength at the center of the stop band.) Thus in designing for a frequency bandwidth $\Delta f/f_0$, the bandwidth w in the formulas is to be set equal to $(\lambda_{g0}/\lambda_0)^2 \Delta f/f_0$ for the narrow bandwidths considered here.

In the waveguide filter each resonator formed from a waveguide of characteristic admittance Y_b, which has a length slightly less than one-half guide wavelength, is connected to the main waveguide of characteristic admittance Y_0 by means of a small elongated coupling iris. Each coupling iris has a length l which is less than one-half free-space wavelength, and can be represented to a good approximation as an inductance in series with the main waveguide. The equivalent circuit of the resonator and coupling iris combination is shown in Fig. 6(d).

The susceptance B of each coupling iris can be determined approximately in terms of the magnetic polarizability, M', of the iris. The expression is[4]

$$\frac{B}{Y_b} = - \frac{\lambda_g ab'}{4\pi M_1'} \quad (36)$$

where a and b' are as defined in Fig. 11. For irises cut in walls of infinitesimal thickness, t, having a length l which is much less than one-half free-space wavelength,

---

[4] H. A. Bethe, "Lumped Constants for Small Irises," Rad. Lab., Cambridge, Mass. Rept. 43-22, M.I.T.; March, 1943.
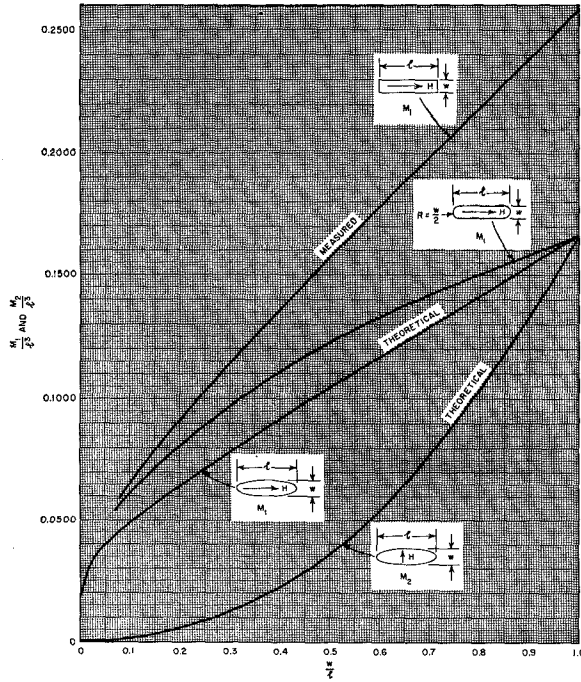
Fig. 12—Magnetic polarizabilities of rectangular,
rounded-end and elliptical slots.

the magnetic polarizability $M_1' = M_1$ is given in Fig. 12.[5]
In the usual situation when t is not infinitesimal and l is
not much less than one-half free-space wavelength, one
must use the magnetic polarizability M_1', which is re-
lated to M_1 by the empirical relation[6]

$$M' = \frac{M_1}{1 - \left(\frac{2l}{\lambda}\right)^2} \times 10^{-(1.36\,t/l)\,[1-(2l/\lambda_0)^2]^{\frac{1}{2}}} \quad (37)$$

where λ_0 is again the free-space wavelength at center
frequency corresponding to $\omega = \omega_0$, $\phi = \phi_0$, and $\lambda_g = \lambda_{g0}$.
The resonant condition for each resonator becomes

$$Y_0 \tan \phi_0 = \frac{Y_b a b'}{4\pi M_1'} \lambda_{g0} \quad (38)$$

where

$$\phi_0 = \frac{2\pi L}{\lambda_{g0}} - \frac{\pi}{2}. \quad (39)$$

The susceptance slope parameter b for each resonator
as viewed from the main transmission line becomes

$$b = \frac{Y_b}{2} G(\phi) \approx Y_b F(\phi) \quad (40)$$

where $F(\phi)$ is defined in (15) and $G(\phi)$ in (17), and M_1'
has been assumed to be frequency invariant.

[5] S. B. Cohn, "Determination of aperture parameters by electro-
lytic-tank measurements," Proc, IRE, vol. 39, pp. 1416–1421;
November, 1951.
[6] S. B. Cohn, "Microwave coupling by large apertures," Proc.
IRE, vol. 40, pp. 696–699; June, 1952.

VIII. EXAMPLE OF WAVEGUIDE FILTER DESIGN

As an example of the use of the above technique, we
consider here the design of a 3-resonator waveguide
band-stop filter using the same low-pass prototype cir-
cuit used for the strip-line filter described in Section VI.
The filter has a design center frequency $f_0 = 10$ Gc and
the resonators and main transmission line are fabricated
from WR-90 waveguide. The fractional bandwidth of
the strip-line filter was $w = 0.05$ on a frequency basis
(34). Here, we use $w = 0.05$ on a reciprocal guide-wave-
length basis (35). The susceptance slope parameters for
the two end resonators and the middle resonator can be
determined from Fig. 4(a) and are, respectively,

$$\frac{b_1}{Y_0} = \frac{b_3}{Y_0} = 12.528$$
$$\frac{b_2}{Y_0} = 18.232 \quad (41)$$

which correspond exactly to those previously computed
for the strip-line filter. The characteristic admittance
Y_b was chosen to be equal to Y_0. Therefore,

$$G(\phi_{01}) = G(\phi_{03}) = \frac{2b_1}{Y_0} = 25.056$$
$$G(\phi_{02}) = \frac{2b_2}{Y_0} = 36.464. \quad (42)$$

Referring to Table II, we find

$$\phi_{01} + 90° = \phi_{03} + 90° = 159.5°$$
$$\phi_{02} + 90° = 163.0°. \quad (43)$$

At a frequency of 10 Gc, λ_{g0} in WR-90 waveguide is
1.5631 inches. Therefore the lengths $L_1 = L_3$ of the two
end resonators and length L_2 of the middle resonator are

$$L_1 = L_3 = 0.693 \text{ inch}$$
$$L_2 = 0.709 \text{ inch}. \quad (44)$$

The magnetic polarizability, $M_{11}' = M_{13}'$, of the irises in
the end cavities and the magnetic polarizability, M_{12}',
of the iris in the middle cavity can be determined from
(37) to be

$$M_{11}' = M_{13}' = 0.0167 \text{ inch}^3$$
$$M_{12}' = 0.0137 \text{ inch}^3. \quad (45)$$

It is convenient to make the iris rectangular in shape
with semicircular ends. Fig. 12 shows that an iris
having $w/l = 0.28$ has $M_1 = 0.0935 \, l^3$. Substitution in
(37) yields values of $l_1 = l_3 \approx 0.43$ inch and $l_2 \approx 0.415$ inch
for iris widths of $w_1 = w_2 = w_3 = 0.12$ inch. Since Bethe's
theory is only approximate, some correction in aper-
ture size may be desirable. The proper correction can be
determined by the experimental procedures discussed
in Section IV.

The waveguide band-stop filter was first assembled so that the outer end walls of the three cavity resonators could be removed to obtain access to the coupling apertures. Then the resonators were tested individually to see whether or not their coupling apertures gave the amount of coupling called for by the theory. This was done by measuring the 3-db bandwidth of one resonator at a time, with aluminum tape covering the apertures to the resonators not being tested. The measured 3-db bandwidth was compared with the values obtained using Fig. 7 in Section IV. The couplings were found to be somewhat loose, and the apertures were lengthened until satisfactory agreement was obtained. All three apertures were 0.120 inch wide; the end apertures were $l_1 = l_3 = 0.481$ inch long while the middle aperture was $l_2 = 0.458$ inch long after final adjustment. The original values computed for these lengths were $l_1 = l_3 = 0.430$ inch and $l_2 = 0.415$ inch. The fact that the final values for the aperture lengths are larger than the computed values is to be expected because in computing $l_1 = l_3$ and l_2, no correction was made for the thickness of the apertures.

After the proper sizes for the coupling apertures were thus established, the end walls were soldered on to the resonators and they were tuned one at a time. This was done by placing aluminum tape on the inside of the guide over the apertures of the resonators not being tuned, and then adjusting the tuning screws on the resonator under test to give maximum insertion loss (typically about 33 db).

The first version of the waveguide band-stop filter had quarter-wavelength spacings between the resonators, and the measured response was as shown in Fig. 13. Instead of one very high peak of attenuation, there were several relatively low peaks. It was found that no matter how the tuning screws on the resonators were adjusted, this situation could not be eliminated. This effect is believed to be due to interaction among the fringing fields in the vicinity of the coupling apertures
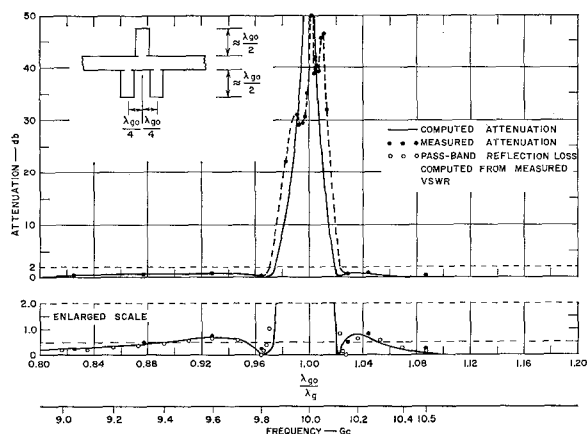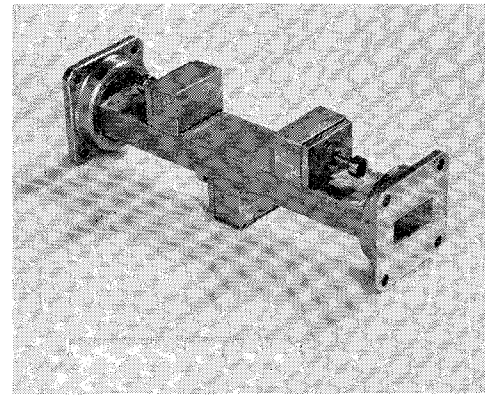

Fig. 14—Three-resonator waveguide band-stop filter using $3\lambda_{g0}/4$ spacings between resonators.
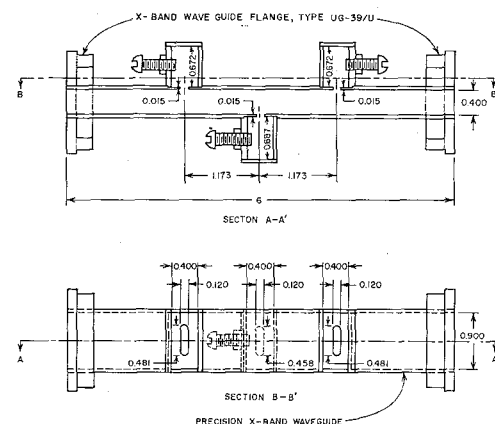

Fig. 15—Dimensions of the waveguide band-stop filter in Fig. 14.

Fig. 13—Computed and measured responses of three-resonator, waveguide, band-stop filter using $\lambda_{g0}/4$ spacings between resonators.
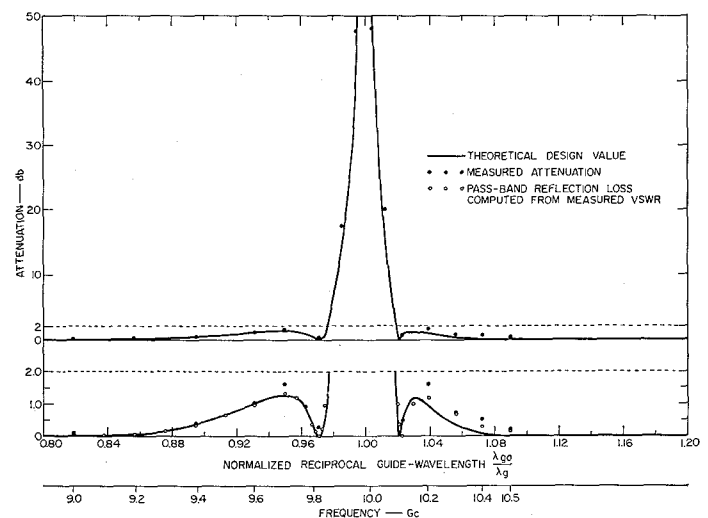

Fig. 16—Computed and measured response of the waveguide band-stop filter in Fig. 14, which has $3\lambda_{g0}/4$ spacings between resonators.

for the various resonators. This problem did not arise in the case of the strip-line band-stop filter, apparently because the stub-to-stub coupling through fringing fields was negligible. (See Section VI.)

In order to circumvent the above-mentioned difficulty, the filter was revised to use three-quarter-wavelength spacings between resonators, instead of quarter-wavelength spacings. The resonator and coupling aperture dimensions were left as before, and the filter was retuned as before. Fig. 14 shows a photograph of the resulting filter, and Fig. 15 shows its dimensions. The computed and measured responses of this filter are shown in Fig. 16, from which it can be seen that the interaction between resonators was eliminated, and the agreement between the computed and measured responses is very close.

IX. CONCLUSIONS

A design procedure has been developed for band-stop filters, suitable for most types of transmission line, from strip line to waveguide. It was shown that a band-stop filter can be derived from a low-pass prototype by means of a frequency transformation, so as to have a stop band of prescribed bandwidth, and equiripple (Chebyshev) or maximally flat (Butterworth) behavior in the pass band. A method was shown by which the lumped-constant resonant circuits can be realized with transmission elements. The theory applies to stop-band bandwidths of up to a few per cent, yielding the predicted stop-band performance very closely, and giving attenuation in the pass band down to dc in one direction, and up to the next stop band in the other direction.

With stubs designated to be near a quarter-wave long at ω_0, this next stop band occurs at three times the frequency of the first (designed) stop band; with stubs designed to be near a one-half wavelength long at ω_0, the second stop band occurs at twice the frequency of the first.

The waveguide band-stop filter in Fig. 15 had a response very close to the response computed for it by calculations that took into account the waveguide size, the inductive coupling of the apertures, etc., as specified by the design equations.

Although the agreement between computed and measured responses is excellent, the filter does not have the 0.5-db Chebyshev pass-band ripple corresponding to the lumped-element, low-pass prototype filter that was used. For instance, in Fig. 16, where three-quarter-wavelength resonators spacings were used, the computed response had about 1.2-db ripple; while in Fig. 13, where one-quarter-wavelength spacing was used between resonators, the ripple was 0.7 db on one side and 0.8 db on the other. In both the case of Fig. 13 and of 16, the over-sized ripples resulted from the selectivity effects of the coupling lines between resonators.

Band-stop filters such as have been described should find numerous applications in microwave systems, where it is desired to suppress or separate a particular band of frequencies without greatly affecting other frequencies nearby.